JOURNAL OF GUIDANCE, CONTROL, AND DYNAMICS
Vol. 22, No. 3, May–June 1999

Sequential Attitude and Attitude-Rate Estimation Using Integrated-Rate Parameters

Yaakov Oshman*
Technion—Israel Institute of Technology, Haifa 32000, Israel
and
F. Landis Markley†
NASA Goddard Space Flight Center, Greenbelt, Maryland 20771

A sequential nonlinear algorithm is presented for gyroless satellite attitude and attitude-rate estimation using vector observations. Based on a third-order, minimal-parameter method for solving the attitude matrix kinematic equation, the resulting estimator is rendered computationally efficient. Employing tracking theory concepts, the angular acceleration is modeled as an exponentially autocorrelated stochastic process, thereby avoiding the use of the typically uncertain spacecraft dynamic model. The estimator's performance is demonstrated via a numerical example, in which it is compared with the estimator implemented onboard the gyroless Solar, Anomalous, and Magnetospheric Particle Explorer spacecraft.

Introduction

SPACECRAFT attitude determination from vector observations has been intensively investigated over the last three decades. In most practical implementations of attitude control systems on gyro-based spacecraft, attitude-rate information is obtained from an onboard triad of rate gyroscopes. This rate information is used in the propagation stage of an attitude estimator, which utilizes noisy vector observations, resolved in both the body-fixed coordinate system and in a reference system, to estimate the spacecraft attitude and gyro drift rates.[1,2]

With the recent advent of accurate, high-bandwidth attitude sensors, the method of attitude determination from vector observations has been extended by several researchers to address the estimation of attitude rate as well, thus facilitating its use on gyroless spacecraft. Gyroless attitude and attitude-rate estimation is, obviously, of prime importance in small, inexpensive spacecraft such as the Solar, Anomalous, Magnetospheric Particle Explorer (SAMPEX), which do not carry gyroscopes but, nevertheless, need to determine their angular velocity for attitude control and attitude propagation purposes.[3] However, even spacecraft that were designed to carry gyroscopes can benefit from the use of attitude-rate estimation in the event of an unexpected gyro failure.[4]

In Ref. 5, high-bandwidth star-tracker measurements were used to solely drive an error-state extended Kalman filter (EKF), which estimates both the spacecraft attitude quaternion and its angular rate. Reference 6 proposed an attitude and attitude-rate estimator, which utilizes temporal derivatives of vector (Earth's magnetic field) measurements and dynamically propagates the angular velocity estimates using the nonlinear Euler's equations. A similar concept was employed in Ref. 7, which introduced an angular-rate estimator (assuming a known attitude), proposing to alleviate the computational complexity normally associated with the Euler equations-based EKF by extending the suboptimal interlaced Kalman filter scheme proposed in Ref. 8. In Ref. 9, predictive filtering was applied to estimate the attitude quaternion in a gyroless setting. Using Euler's equations (assuming that the spacecraft dynamic model is accurately known), the attitude rate was estimated as a byproduct from the estimated spacecraft angular momentum.

A major disadvantage of model-based estimation methods is that this model is frequently highly uncertain and typically renders the resulting estimator computationally burdensome and sensitive to uncertainties in the spacecraft parameters,[10] e.g., the spacecraft inertia tensor, momentum wheel dynamic model, and thruster pressure-thrust calibration. The inherent difficulty in obtaining accurate spacecraft dynamic models has been well recognized in previous works. Thus, Ref. 11 proposed a method, based on the batch minimum model error estimator, which can estimate the attitude of a poorly modeled spacecraft and, moreover, can be used to generate a dynamic model for the system in a postestimation analysis. In Ref. 12, the attitude and attitude-rate estimator utilized the spacecraft dynamic model, but the disturbance torque (representing a variety of unmodeled effects, e.g., atmospheric drag, solar radiation pressure, etc.) was stochastically modeled as a random-walk process. Reference 6, while also employing the Euler's equations formulation, suggested solving the associated uncertainty problem by modeling the inherent rate errors using a first-order Markov model.

The algorithm proposed in the present work simultaneously estimates both the attitude matrix and the spacecraft angular velocity from vector measurements, using a third-order attitude parameterization based on the integrated-rate parameters (IRP).[13] In contrast with previous model-based estimation methods, the approach taken here makes no use of the spacecraft dynamic model. Instead, time propagation of the estimated variables is performed in the proposed filter by modeling the spacecraft angular acceleration as an exponentially autocorrelated stochastic process and using a polynomial kinematic model, a concept borrowed from tracking theory,[14] where it has been widely used to estimate the motion of noncooperative targets. A similar, but simpler, approach was employed for the Applied Technology Satellite 6 (Ref. 15). Extending the approach of Ref. 16, in which vector measurements were used to estimate the attitude of a gyro-based spacecraft, the present work also differs from previous work in the following two respects. First, the acquired vector measurements are directly processed to extract attitude and attitude-rate information, thus avoiding the precomputation of temporal derivatives of these noisy measurements, as required by some other filtering schemes.[7,17] Second, in contrast with other methods relying mainly on the attitude quaternion, the algorithm presented here directly estimates the attitude matrix, a natural, nonsingular attitude representation. Building on the minimal IRP third-order parameterization, the new estimator assigns just three state variables

Received Jan. 26, 1998; revision received July 28, 1998; presented as Paper 98-4508 at the AIAA Guidance, Navigation, and Control Conference, Boston, MA, Aug. 10–12, 1998; accepted for publication Aug. 18, 1998. Copyright © 1998 by the American Institute of Aeronautics and Astronautics, Inc. No copyright is asserted in the United States under Title 17, U.S. Code. The U.S. Government has a royalty-free license to exercise all rights under the copyright claimed herein for Governmental purposes. All other rights are reserved by the copyright owner.

*Associate Professor, Department of Aerospace Engineering. Associate Fellow, AIAA.
†Staff Engineer, Guidance, Navigation, and Control Center, Code 571. Fellow AIAA.

for the estimation of the nine-parameter attitude matrix, which is at the heart of its computational efficiency.

In the following section we briefly review the IRP method for the solution of the attitude evolution equation. This is followed by a presentation of the angular acceleration kinematic model. The filtering stage of the estimator is then developed, applying minimum mean-squared error estimation theory to a perturbation model, obtained by linearizing the observation equation about the predicted state. An attitude matrix orthogonalization procedure, incorporated to enhance the algorithm's accuracy and robustness, is then discussed, followed by a presentation of the estimator's prediction stage. The algorithm's performance is demonstrated via a numerical example, in which it is compared with the performance of the estimator used in the SAMPEX spacecraft. Concluding remarks are offered in the last section.

Integrated-Rate Parameters

Consider the matrix differential equation

$$\dot{V}(t) = W(t)V(t), \qquad V(t_0) = V_0 \tag{1}$$

where $V(t) \in \mathbb{R}^{n,n}$, $W(t) = -W^T(t)$ for all $t \geq t_0$, $V_0 V_0^T = I$, and the overdot indicates the temporal derivative. This equation arises naturally in three-dimensional attitude determination problems, as well as in the square-root solution of the matrix differential Riccati equation.[18] Let the skew-symmetric matrix $A(t, t_0)$ be defined as

$$A(t, t_0) \triangleq \int_{t_0}^{t} W(\tau)\, \mathrm{d}\tau \tag{2}$$

Then, a third-order, minimal-parameter solution of Eq. (1) [using only the $m = n(n-1)/2$ off-diagonal terms of $A(t, t_0)$] is[13]

$$\tilde{V}(t, t_0) \triangleq \left\{ I + A(t, t_0) + \frac{A^2(t, t_0)}{2!} + \frac{A^3(t, t_0)}{3!} + \frac{(t - t_0)}{3!}[A(t, t_0)W_0 - W_0 A(t, t_0)] \right\} V_0 \tag{3}$$

where $W_0 = W(t_0)$.

In the three-dimensional case, the off-diagonal entries of $A(t, t_0)$, termed IRPs, are the angles resulting from a temporal integration of the three components of the angular velocity vector $\boldsymbol{\omega}(t) \triangleq [\omega_1(t) \;\; \omega_2(t) \;\; \omega_3(t)]^T$, where ω_i is the angular velocity component along the i axis of the initial coordinate system and $i = 1, 2, 3$ for x, y, z, respectively.

Remark 1. The distinction between the IRP and Euler angles should be emphasized. Unlike the latter, the IRP set can only serve as an approximate, third-order attitude parameterization [in the sense of Eq. (3)], and, hence, the parameters' usefulness depends on their size. In the filtering algorithm presented in this work, the size of the IRP vector is controlled by proper selection of the filter's sampling interval and, as will be shown in the sequel, by applying reset control.

Notice that in Eq. (3) the approximate solution $\tilde{V}(t, t_0)$ is computed using the matrix W evaluated at t_0. For the sake of the ensuing development, it will prove useful to derive an alternative third-order solution, which is directly based on $W(t)$.

Theorem 1. Let the matrix-valued function $\bar{W}_0(t)$ be defined as

$$\bar{W}_0(t) \triangleq W(t) - (t - t_0)\dot{W}(t) \tag{4}$$

Then, the following matrix-valued function is a third-order approximation of $V(t)$:

$$\tilde{V}_1(t, t_0) \triangleq \left\{ I + A(t, t_0) + \frac{A^2(t, t_0)}{2!} + \frac{A^3(t, t_0)}{3!} + \frac{t - t_0}{3!}[A(t, t_0)\bar{W}_0(t) - \bar{W}_0(t)A(t, t_0)] \right\} V_0 \tag{5}$$

Proof. To obtain Eq. (5), the following Taylor's expansion for W_0:

$$W_0 = W(t) - \dot{W}(t)(t - t_0) + \mathcal{O}\left[(t - t_0)^2\right] \tag{6}$$

is used in the commutator term of Eq. (3).

That $\tilde{V}_1(t, t_0)$ constitutes a third-order approximation of the solution is proven by showing that all of the derivatives of this function up to order three are equal to the corresponding derivatives of the exact solution at t_0. This can be done by a straightforward, albeit tedious, direct comparison of the first three derivatives of $V(t)$ and $\tilde{V}_1(t, t_0)$ at t_0. □

In the three-dimensional case, the orthogonal matrix differential equation (1) is rewritten as

$$\dot{D}(t) = \Omega(t)D(t), \qquad D(t_0) = D_0 \tag{7}$$

where $D(t)$ is the attitude matrix, or the direction cosine matrix (DCM), $\Omega(t) = -[\boldsymbol{\omega}(t)\times]$, and $[\boldsymbol{\omega}(t)\times]$ is the usual cross product matrix corresponding to $\boldsymbol{\omega}(t)$. In this case, the matrix $A(t, t_0)$ takes the form

$$A(t, t_0) \triangleq -[\boldsymbol{\theta}(t)\times] \tag{8}$$

where the parameter vector $\boldsymbol{\theta}(t)$ is defined as

$$\boldsymbol{\theta}(t) \triangleq [\theta_1(t) \quad \theta_2(t) \quad \theta_3(t)]^T \tag{9}$$

and

$$\theta_i(t) \triangleq \int_{t_0}^{t} \omega_i(\tau)\, \mathrm{d}\tau, \qquad i = 1, 2, 3 \tag{10}$$

Now let the sampling period be denoted by $T \triangleq t_{k+1} - t_k$. Using the notation $\boldsymbol{\theta}(k) \triangleq \boldsymbol{\theta}(t_k)$, the parameter vector at time t_k is

$$\boldsymbol{\theta}(k) = [\theta_1(k) \quad \theta_2(k) \quad \theta_3(k)]^T \tag{11}$$

and Eq. (10) implies

$$\theta_i(k) = \int_{t_0}^{t_k} \omega_i(\tau)\, \mathrm{d}\tau, \qquad i = 1, 2, 3 \tag{12}$$

From Eq. (12) we have

$$\boldsymbol{\theta}(k + 1) = \boldsymbol{\theta}(k) + \int_{t_k}^{t_{k+1}} \boldsymbol{\omega}(\tau)\, \mathrm{d}\tau \tag{13}$$

Defining $A(k + 1, k)$ to be the discrete-time analog of $A(t, t_0)$, i.e.,

$$A(k + 1, k) \triangleq -[(\boldsymbol{\theta}(k + 1) - \boldsymbol{\theta}(k))\times] \tag{14}$$

Eq. (3) is rewritten as

$$D(k + 1) = \left\{ I + A(k + 1, k) + \tfrac{1}{2}A^2(k + 1, k) + \tfrac{1}{6}A^3(k + 1, k) + \tfrac{1}{6}T[A(k + 1, k)\Omega(k) - \Omega(k)A(k + 1, k)] \right\} D(k) \tag{15}$$

Similarly, let $\dot{\Omega}(k + 1) \triangleq -[\dot{\boldsymbol{\omega}}(k + 1)\times]$ and $\Psi(k + 1) \triangleq -[\boldsymbol{\psi}(k + 1)\times]$, where

$$\boldsymbol{\psi}(k + 1) \triangleq \boldsymbol{\omega}(k + 1) - \dot{\boldsymbol{\omega}}(k + 1)T \tag{16}$$

Then the corresponding discrete-time equivalent of Eq. (5) is

$$D(k + 1) = \left\{ I + A(k + 1, k) + \tfrac{1}{2}A^2(k + 1, k) + \tfrac{1}{6}A^3(k + 1, k) + \tfrac{1}{6}T[A(k + 1, k)\Psi(k + 1) - \Psi(k + 1)A(k + 1, k)] \right\} D(k) \tag{17}$$

Kinematic Motion Model

To avoid using the uncertain spacecraft dynamic model, we treat the spacecraft as a noncooperative target whose motion is to be tracked by our estimator. Using this approach, the attitude/attitude-rate estimator to be developed in the sequel becomes a motion tracker. To develop our estimator we can, therefore, use any of the many methods that have been developed over the years in the tracking theory area. In this work we have chosen the Singer time-correlated maneuvering-acceleration model, proposed in 1970 for the purpose of estimating the states of maneuvering targets.[14] According to this model, which has been one of the foundations in the area of maneuvering target tracking (e.g., air-to-air missile vs aircraft scenario) since its introduction,[19,20] the target acceleration is modeled as a zero-mean, exponentially autocorrelated stochastic

process. It should be noted that, although more sophisticated models, which have been developed over the years,[20,21] could have been used for the purpose of the present work, the Singer model has been chosen here to simplify the ensuing development and clarify the main approach.

Using the Singer model, then, the angular acceleration kinematic model is the following first-order Markov process:

$$\ddot{\boldsymbol{\omega}}(t) = -\Lambda\dot{\boldsymbol{\omega}}(t) + \tilde{\boldsymbol{\nu}}(t) \tag{18}$$

For simplicity, a decoupled kinematic model is chosen for the three angular-rate components, i.e.,

$$\Lambda \triangleq \operatorname{diag}\{1/\tau_1,\, 1/\tau_2,\, 1/\tau_3\} \tag{19}$$

where $\{\tau_i\}_{i=1}^3$ are the acceleration decorrelation times along the corresponding body axes (a more elaborate model can be used, as a simple extension of the present approach). The driving noise is a zero-mean white process, with

$$E\{\tilde{\boldsymbol{\nu}}(t)\tilde{\boldsymbol{\nu}}^T(s)\} = \tilde{Q}(t)\delta(t-s) \tag{20}$$

and the power spectral density matrix is

$$\tilde{Q}(t) = 2\Lambda\Sigma^2 \tag{21}$$

where

$$\Sigma \triangleq \operatorname{diag}\{\sigma_1, \sigma_2, \sigma_3\} \tag{22}$$

To determine the noise variances in Eq. (22), the Singer acceleration probabilistic model is used[14]: The angular acceleration components $\{\dot{\omega}_i\}_{i=1}^3$ can be 1) equal to $\dot{\omega}_{M_i}$ with probability p_{M_i}, 2) equal to $-\dot{\omega}_{M_i}$ with probability p_{M_i}, 3) equal to zero with probability p_{0_i}, or 4) uniformly distributed over the interval $[-\dot{\omega}_{M_i}, \dot{\omega}_{M_i}]$ with the remaining probability mass. Using this model, it follows that

$$\sigma_i^2 = \left(\dot{\omega}_{M_i}^2/3\right)\left(1 + 4p_{M_i} - p_{0_i}\right) \tag{23}$$

Remark 2. The parameters $\dot{\omega}_{M_i}$, p_{M_i}, and p_{0_i} are considered tuning parameters. As is customarily done, they are selected before the mission by experience with real and simulated data, so as to tune the filter to match the characteristics of the specific problem. However, we note that adaptive tracking algorithms can be used that automatically adapt the model parameters on-the-fly.[21]

Now let the system's state vector be defined as

$$\boldsymbol{x}(t) \triangleq [\boldsymbol{\theta}^T(t) \quad \boldsymbol{\omega}^T(t) \quad \dot{\boldsymbol{\omega}}^T(t)]^T \tag{24}$$

then the state equation is

$$\dot{\boldsymbol{x}}(t) = F\boldsymbol{x}(t) + \tilde{\boldsymbol{\nu}}(t) \equiv \begin{bmatrix} 0 & I & 0 \\ 0 & 0 & I \\ 0 & 0 & -\Lambda \end{bmatrix}\boldsymbol{x}(t) + \begin{bmatrix} 0 \\ 0 \\ \tilde{\nu}(t) \end{bmatrix} \tag{25}$$

with obvious definitions of F and $\tilde{\boldsymbol{\nu}}(t)$. Corresponding to the sampling interval T, the discrete-time state equation is

$$\boldsymbol{x}(k+1) = \Phi(T)\boldsymbol{x}(k) + \boldsymbol{\nu}(k) \tag{26}$$

where the transition matrix is

$$\Phi(T) \equiv e^{FT} = \begin{bmatrix} I & TI & \Lambda^{-2}(e^{-\Lambda T} - I + T\Lambda) \\ 0 & I & \Lambda^{-1}(I - e^{-\Lambda T}) \\ 0 & 0 & e^{-\Lambda T} \end{bmatrix} \tag{27}$$

and $\boldsymbol{\nu}(k)$ is a zero-mean, white noise sequence, with covariance

$$Q(k) \triangleq E\{\boldsymbol{\nu}(k)\boldsymbol{\nu}^T(k)\} = \int_0^T e^{F(T-t)}\operatorname{diag}\{0, 0, \tilde{Q}(t)\}e^{F^T(T-t)}\,\mathrm{d}t \tag{28}$$

Explicit computation of the integrals in Eq. (28) yields the following expressions for the entries of the symmetric covariance matrix $Q(k)$:

$$Q_{11}(k) = \Lambda^{-4}\Sigma^2\left(I + 2\Lambda T - 2\Lambda^2T^2 + \tfrac{2}{3}\Lambda^3T^3 - e^{-2\Lambda T} - 4\Lambda T e^{-\Lambda T}\right) \tag{29a}$$

$$Q_{12}(k) = \Lambda^{-3}\Sigma^2(I - 2\Lambda T + \Lambda^2T^2 - 2e^{-\Lambda T} + e^{-2\Lambda T} + 2\Lambda T e^{-\Lambda T}) \tag{29b}$$

$$Q_{13}(k) = \Lambda^{-2}\Sigma^2(I - e^{-2\Lambda T} - 2\Lambda T e^{-\Lambda T}) \tag{29c}$$

$$Q_{22}(k) = \Lambda^{-2}\Sigma^2(4e^{-\Lambda T} - 3I - e^{-2\Lambda T} + 2\Lambda T) \tag{29d}$$

$$Q_{23}(k) = \Lambda^{-1}\Sigma^2(e^{-2\Lambda T} + I - 2e^{-\Lambda T}) \tag{29e}$$

$$Q_{33}(k) = \Sigma^2(I - e^{-2\Lambda T}) \tag{29f}$$

Measurement Processing

Assume that at t_{k+1} we have on hand the minimum-mean-squared error (MMSE) predicted vector $\hat{\boldsymbol{x}}(k+1\,|\,k)$ and its corresponding prediction error covariance matrix $P(k+1\,|\,k) \triangleq E\{\tilde{\boldsymbol{x}}(k+1\,|\,k)\tilde{\boldsymbol{x}}^T(k+1\,|\,k)\}$, where the estimation error is defined as

$$\tilde{\boldsymbol{x}}(j\,|\,k) \triangleq \boldsymbol{x}(j) - \hat{\boldsymbol{x}}(j\,|\,k) \tag{30}$$

As the first step in developing the measurement update algorithm, we next formulate the observation equation, relating the acquired vector measurements to the state.

Observation Statistical Model

Let a new pair of corresponding noisy vector measurements be acquired at t_{k+1}. This pair consists of the unit vectors $\boldsymbol{u}(k+1)$ and $\boldsymbol{v}(k+1)$, which represent the realizations of the same vector as modeled in the reference coordinate system and measured in the body coordinate system, respectively. The direction-cosine matrix $D(k+1)$, representing the true attitude of the body coordinate system relative to the reference system at time t_{k+1}, transforms the true vector representation $\boldsymbol{u}_0$ in the reference coordinate system into its corresponding true representation $\boldsymbol{v}_0$ in the body coordinate system according to

$$\boldsymbol{v}_0(k+1) = D(k+1)\boldsymbol{u}_0(k+1) \tag{31}$$

Assuming no constraint on the measurement noise direction, the body-frame measured unit vector $\boldsymbol{v}(k+1)$ is related to the true vector according to

$$\boldsymbol{v}(k+1) = \frac{\boldsymbol{v}_0(k+1) + \boldsymbol{n}_v'(k+1)}{\|\boldsymbol{v}_0(k+1) + \boldsymbol{n}_v'(k+1)\|} \tag{32}$$

where $\boldsymbol{n}_v'(k+1) \sim \mathcal{N}(0, R_v'(k+1))$ is the white sensor measurement noise. Because both $\boldsymbol{v}_0(k+1)$ and $\boldsymbol{v}(k+1)$ are unit vectors, it follows from Eq. (32) that

$$\boldsymbol{v}(k+1) = \boldsymbol{v}_0(k+1) + \boldsymbol{n}_v(k+1) \tag{33}$$

where $\boldsymbol{n}_v(k+1) \triangleq \mathcal{P}_{v_0}^{\perp}(k+1)\boldsymbol{n}_v'(k+1) \sim \mathcal{N}[0, R_v(k+1)]$ is the effective white measurement noise, $\mathcal{P}_{v_0}^{\perp}(k+1) \triangleq I - \boldsymbol{v}_0(k+1)\boldsymbol{v}_0^T(k+1)$ is the orthogonal projector onto the orthogonal complement of span$\{\boldsymbol{v}_0(k+1)\}$, and the measurement noise covariance matrix is

$$R_v(k+1) \triangleq \mathcal{P}_{v_0}^{\perp}(k+1)R_v'(k+1)\mathcal{P}_{v_0}^{\perp}(k+1) \tag{34}$$

To account for nonideal effects, e.g., star catalog errors, it is assumed that the measured reference vector is related to the true vector according to

$$\boldsymbol{u}(k+1) = \boldsymbol{u}_0(k+1) + \boldsymbol{n}_u(k+1) \tag{35}$$

where $\boldsymbol{n}_u \perp \boldsymbol{u}_0$ is a white measurement noise that is uncorrelated with $\boldsymbol{n}_v$ and satisfies $\boldsymbol{n}_u(k) \sim \mathcal{N}[0, R_u(k)]$, with $R_u(k)$ being a known covariance matrix.

Measurement Linearization

To relate the information contained in the measurements to the state vector at t_{k+1}, Eq. (31) is rewritten as

$$\boldsymbol{v}_0(k+1) = D[\boldsymbol{\theta}(k+1) - \boldsymbol{\theta}(k), \boldsymbol{\omega}(k+1), \dot{\boldsymbol{\omega}}(k+1), D(k)]\boldsymbol{u}_0(k+1) \tag{36}$$

where the notation reflects that by Eqs. (14), (16), and (17) the attitude at time t_{k+1} is related to the attitude at time t_k via the IRP

vector difference $\boldsymbol{\theta}(k+1) - \boldsymbol{\theta}(k)$, the angular rate $\boldsymbol{\omega}(k+1)$, and the angular acceleration $\dot{\boldsymbol{\omega}}(k+1)$.

To process the information contained in the new vector measurements, the nonlinear measurement Eq. (36) is next linearized about a nominal state, consisting of the most recent estimates. Assuming that after the previous measurement update (at t_k) linearization has been performed about the a posteriori state estimate, the resulting nominal state vector at t_{k+1} is the predicted estimate $\hat{\boldsymbol{x}}(k+1\,|\,k)$. Therefore, the predicted state vector is assumed to be related to the true one according to

$$\begin{aligned}\boldsymbol{x}(k+1) &= \hat{\boldsymbol{x}}(k+1\,|\,k) + \delta\boldsymbol{x}(k+1)\\ &\equiv \begin{bmatrix}\hat{\boldsymbol{\theta}}(k+1\,|\,k)\\ \hat{\boldsymbol{\omega}}(k+1\,|\,k)\\ \hat{\dot{\boldsymbol{\omega}}}(k+1\,|\,k)\end{bmatrix} + \begin{bmatrix}\delta\boldsymbol{\theta}(k+1)\\ \delta\boldsymbol{\omega}(k+1)\\ \delta\dot{\boldsymbol{\omega}}(k+1)\end{bmatrix}\end{aligned} \tag{37}$$

where $\delta\boldsymbol{\theta}(k+1)$, $\delta\boldsymbol{\omega}(k+1)$, and $\delta\dot{\boldsymbol{\omega}}(k+1)$ are the perturbations of the state components about the nominal, i.e., predicted, state. Let $\hat{D}^*(k\,|\,k)$ denote the a posteriori, orthogonalized estimate of the attitude matrix at time t_k, to be discussed in the sequel. Using now the most recent estimates for $D(k)$ and $\boldsymbol{x}(k)$, namely, $\hat{D}^*(k\,|\,k)$ and $\hat{\boldsymbol{x}}(k\,|\,k)$, respectively, in Eq. (36), it follows from Eqs. (33), (35), and (37) that

$$\begin{aligned}\boldsymbol{v}(k+1) - \boldsymbol{n}_v(k+1) &= D[\hat{\boldsymbol{\theta}}(k+1\,|\,k) + \delta\boldsymbol{\theta}(k+1)\\ &\quad - \hat{\boldsymbol{\theta}}(k\,|\,k), \hat{\boldsymbol{\omega}}(k+1\,|\,k) + \delta\boldsymbol{\omega}(k+1), \hat{\dot{\boldsymbol{\omega}}}(k+1\,|\,k)\\ &\quad + \delta\dot{\boldsymbol{\omega}}(k+1), \hat{D}^*(k\,|\,k)][\boldsymbol{u}(k+1) - \boldsymbol{n}_u(k+1)]\end{aligned} \tag{38}$$

As discussed in the sequel, the a posteriori IRP estimate is zeroed after each measurement update (due to full reset control of the IRP state). We will, therefore, use the reset value of the IRP estimate, $\hat{\boldsymbol{\theta}}^c(k\,|\,k) = 0$, in Eq. (38). Now expand D about the nominal state using a first-order Taylor series expansion, i.e.,

$$\begin{aligned}&D[\hat{\boldsymbol{\theta}}(k+1\,|\,k) + \delta\boldsymbol{\theta}(k+1), \hat{\boldsymbol{\omega}}(k+1\,|\,k) + \delta\boldsymbol{\omega}(k+1), \hat{\dot{\boldsymbol{\omega}}}(k+1\,|\,k) + \delta\dot{\boldsymbol{\omega}}(k+1), \hat{D}^*(k\,|\,k)]\\ &= \hat{D}(k+1\,|\,k) + \sum_{i=1}^{3} \left.\frac{\partial D[\boldsymbol{\theta}(k+1), \hat{\boldsymbol{\omega}}(k+1\,|\,k), \hat{\dot{\boldsymbol{\omega}}}(k+1\,|\,k), \hat{D}^*(k\,|\,k)]}{\partial\theta_i}\right|_{\hat{\boldsymbol{\theta}}(k+1\,|\,k)} \delta\theta_i(k+1)\\ &\quad + \sum_{i=1}^{3} \left.\frac{\partial D[\hat{\boldsymbol{\theta}}(k+1\,|\,k), \boldsymbol{\omega}(k+1), \hat{\dot{\boldsymbol{\omega}}}(k+1\,|\,k), \hat{D}^*(k\,|\,k)]}{\partial\omega_i}\right|_{\hat{\boldsymbol{\omega}}(k+1\,|\,k)} \delta\omega_i(k+1)\\ &\quad + \sum_{i=1}^{3} \left.\frac{\partial D[\hat{\boldsymbol{\theta}}(k+1\,|\,k), \hat{\boldsymbol{\omega}}(k+1\,|\,k), \dot{\boldsymbol{\omega}}(k+1), \hat{D}^*(k\,|\,k)]}{\partial\dot{\omega}_i}\right|_{\hat{\dot{\boldsymbol{\omega}}}(k+1\,|\,k)} \delta\dot{\omega}_i(k+1)\end{aligned} \tag{39}$$

where $(\,)|_\zeta$ denotes evaluated at ζ and

$$\begin{aligned}&\hat{D}(k+1\,|\,k)\\ &\triangleq D[\hat{\boldsymbol{\theta}}(k+1\,|\,k), \hat{\boldsymbol{\omega}}(k+1\,|\,k), \hat{\dot{\boldsymbol{\omega}}}(k+1\,|\,k), \hat{D}^*(k\,|\,k)]\end{aligned} \tag{40}$$

Differentiating Eq. (17), the sensitivity matrices appearing in Eq. (39) are computed as

$$\begin{aligned}&\frac{\partial}{\partial\theta_i} D[\boldsymbol{\theta}(k+1), \hat{\boldsymbol{\omega}}(k+1\,|\,k), \hat{\dot{\boldsymbol{\omega}}}(k+1\,|\,k), \hat{D}^*(k\,|\,k)]\\ &= G_i[\boldsymbol{\theta}(k+1), \hat{\boldsymbol{\psi}}(k+1\,|\,k)]\hat{D}^*(k\,|\,k)\end{aligned} \tag{41a}$$

$$\begin{aligned}&\frac{\partial}{\partial\omega_i} D[\hat{\boldsymbol{\theta}}(k+1\,|\,k), \boldsymbol{\omega}(k+1), \hat{\dot{\boldsymbol{\omega}}}(k+1\,|\,k), \hat{D}^*(k\,|\,k)]\\ &= \frac{1}{6} T F_i[\hat{\boldsymbol{\theta}}(k+1\,|\,k)]\hat{D}^*(k\,|\,k)\end{aligned} \tag{41b}$$

$$\begin{aligned}&\frac{\partial}{\partial\dot{\omega}_i} D[\hat{\boldsymbol{\theta}}(k+1\,|\,k), \hat{\boldsymbol{\omega}}(k+1\,|\,k), \dot{\boldsymbol{\omega}}(k+1), \hat{D}^*(k\,|\,k)]\\ &= -\frac{1}{6} T^2 F_i[\hat{\boldsymbol{\theta}}(k+1\,|\,k)]\hat{D}^*(k\,|\,k)\end{aligned} \tag{41c}$$

for $i = 1, 2, 3$, where $\hat{\boldsymbol{\psi}}(k+1\,|\,k) \triangleq \hat{\boldsymbol{\omega}}(k+1\,|\,k) - T\hat{\dot{\boldsymbol{\omega}}}(k+1\,|\,k)$ and the sensitivity matrices $\{G_i, F_i\}_{i=1}^3$ are

$$\begin{aligned}G_i(\boldsymbol{\theta}, \boldsymbol{\psi}) &= \tfrac{1}{2}\left(\boldsymbol{\theta}\boldsymbol{e}_i^T + \boldsymbol{e}_i\boldsymbol{\theta}^T\right) - \boldsymbol{\theta}_i I - \left(1 - \tfrac{1}{6}\|\boldsymbol{\theta}\|^2\right)[\boldsymbol{e}_i\times]\\ &\quad + \tfrac{1}{6} T\left(\boldsymbol{\psi}\boldsymbol{e}_i^T - \boldsymbol{e}_i\boldsymbol{\psi}^T\right) + \tfrac{1}{3}\boldsymbol{\theta}_i[\boldsymbol{\theta}\times]\end{aligned} \tag{42a}$$

$$F_i(\boldsymbol{\theta}) = \boldsymbol{e}_i\boldsymbol{\theta}^T - \boldsymbol{\theta}\boldsymbol{e}_i^T \tag{42b}$$

where $\boldsymbol{e}_i$ is the unit vector on the ith axis, $i = 1, 2, 3$.

Remark 3. In a typical application, it can be assumed that the parameters $\{\theta_i\}_{i=1}^3$ are small, such that the second-order quantities $\{\theta_i\theta_j\}_{i,j=1}^3$ are negligible in Eq. (42a). Using this small-angle approximation results in much simpler forms for $G_i(\boldsymbol{\theta}, \boldsymbol{\psi})$. The actual use of either Eq. (42a) or its small-angle approximation depends, in practice, on the dynamics of the specific application.

Using Eq. (39) in Eq. (38) and neglecting second-order terms yields

$$\begin{aligned}\boldsymbol{v}(k+1) - \hat{D}(k+1\,|\,k)\boldsymbol{u}(k+1) &= H(k+1)\delta\boldsymbol{x}(k+1)\\ &\quad - \hat{D}(k+1\,|\,k)\boldsymbol{n}_u(k+1) + \boldsymbol{n}_v(k+1)\end{aligned} \tag{43}$$

where the observation matrix $H(k+1)$ is written in block matrix form as

$$H(k+1) \equiv [H_1(k+1) \quad H_2(k+1) \quad H_3(k+1)] \tag{44}$$

and the columns of the submatrices $H_i(k+1) \in \mathbb{R}^{3,3}$, $i = 1, 2, 3$, are

$$H_{1j}(k+1) = G_j[\hat{\boldsymbol{\theta}}(k+1\,|\,k), \hat{\boldsymbol{\psi}}(k+1\,|\,k)]\hat{D}^*(k\,|\,k)\boldsymbol{u}(k+1) \tag{45a}$$

$$H_{2j}(k+1) = \tfrac{1}{6} T F_j[\hat{\boldsymbol{\theta}}(k+1\,|\,k)]\hat{D}^*(k\,|\,k)\boldsymbol{u}(k+1) \tag{45b}$$

$$H_{3j}(k+1) = -T H_{2j}(k+1) \tag{45c}$$

for $j = 1, 2, 3$. Define now the effective measurement and measurement noise to be, respectively,

$$\boldsymbol{y}(k+1) \triangleq \boldsymbol{v}(k+1) - \hat{D}(k+1\,|\,k)\boldsymbol{u}(k+1) \tag{46}$$

$$\boldsymbol{n}(k+1) \triangleq \boldsymbol{n}_v(k+1) - \hat{D}(k+1\,|\,k)\boldsymbol{n}_u(k+1) \tag{47}$$

Then, using these definitions in Eq. (43) yields the following measurement equation:

$$\boldsymbol{y}(k+1) = H(k+1)\delta\boldsymbol{x}(k+1) + \boldsymbol{n}(k+1) \tag{48}$$

The white measurement noise is $\boldsymbol{n}(k+1) \sim \mathcal{N}[0, R(k+1)]$ where

$$R(k+1) \triangleq R_v(k+1) + \hat{D}(k+1\,|\,k)R_u(k+1)\hat{D}^T(k+1\,|\,k) \tag{49}$$

Measurement Update

From Eqs. (30) and (37) it follows that

$$\delta \boldsymbol{x}(k+1) = \boldsymbol{x}(k+1) - \hat{\boldsymbol{x}}(k+1\,|\,k) = \tilde{\boldsymbol{x}}(k+1\,|\,k) \tag{50}$$

Because $\hat{\boldsymbol{x}}(k+1\,|\,k)$ is an unbiased, MMSE predictor, we have

$$E\{\delta \boldsymbol{x}(k+1)\} = E\{\tilde{\boldsymbol{x}}(k+1\,|\,k)\} = 0 \tag{51}$$

and

$$\operatorname{cov}\{\delta \boldsymbol{x}(k+1)\} = \operatorname{cov}\{\tilde{\boldsymbol{x}}(k+1\,|\,k)\} = P(k+1\,|\,k) \tag{52}$$

yielding

$$\delta \boldsymbol{x}(k+1) \sim \mathcal{N}[0,\, P(k+1\,|\,k)] \tag{53}$$

Using the linearized measurement equation (48) and the statistical properties of the measurement and prediction errors, the MMSE estimator of $\delta \boldsymbol{x}(k+1)$ is

$$\widehat{\delta \boldsymbol{x}}(k+1\,|\,k+1) = K(k+1)\boldsymbol{y}(k+1) \tag{54}$$

where $K(k+1)$, the estimator gain matrix, is computed as

$$K(k+1) = P(k+1\,|\,k)H^T(k+1) \times [H(k+1)P(k+1\,|\,k)H^T(k+1) + R(k+1)]^{-1} \tag{55}$$

Also, from Eq. (50) we have

$$\widehat{\delta \boldsymbol{x}}(k+1\,|\,k+1) = \hat{\boldsymbol{x}}(k+1\,|\,k+1) - \hat{\boldsymbol{x}}(k+1\,|\,k) \tag{56}$$

which, used in Eq. (54), yields the state measurement update equation

$$\hat{\boldsymbol{x}}(k+1\,|\,k+1) = \hat{\boldsymbol{x}}(k+1\,|\,k) + K(k+1)\boldsymbol{y}(k+1) \tag{57}$$

To derive the covariance update equation, subtract $\boldsymbol{x}(k+1)$ from both sides of the last equation and use Eqs. (48) and (50) to obtain

$$\tilde{\boldsymbol{x}}(k+1\,|\,k+1) = [I - K(k+1)H(k+1)]\tilde{\boldsymbol{x}}(k+1\,|\,k) - K(k+1)\boldsymbol{n}(k+1) \tag{58}$$

from which the resulting covariance update equation is

$$P(k+1\,|\,k+1) = [I - K(k+1)H(k+1)] \times P(k+1\,|\,k)[I - K(k+1)H(k+1)]^T + K(k+1)R(k+1)K^T(k+1) \tag{59}$$

where the filtering error covariance matrix $P(k+1\,|\,k+1)$ is

$$P(k+1\,|\,k+1) \triangleq E[\tilde{\boldsymbol{x}}(k+1\,|\,k+1)\tilde{\boldsymbol{x}}^T(k+1\,|\,k+1)] \tag{60}$$

To compute the measurement-updated attitude matrix at time t_{k+1}, we use the most recent estimate $\hat{\boldsymbol{x}}(k+1\,|\,k+1)$ and the estimated attitude matrix corresponding to time t_k in Eq. (17). This yields

$$\hat{D}(k+1\,|\,k+1) = \Big\{I + \hat{A}(k+1,k) + \tfrac{1}{2}\hat{A}^2(k+1,k) + \tfrac{1}{6}\hat{A}^3(k+1,k) + \tfrac{1}{6}T[\hat{A}(k+1,k)\hat{\Psi}(k+1\,|\,k+1) - \hat{\Psi}(k+1\,|\,k+1)\hat{A}(k+1,k)]\Big\}\hat{D}^*(k\,|\,k) \tag{61}$$

where the a posteriori estimates of $A(k+1,k)$ and $\Psi(k+1)$ are defined, respectively, as

$$\hat{A}(k+1,k) \triangleq -[\hat{\boldsymbol{\theta}}(k+1\,|\,k+1)\times] \tag{62}$$

$$\hat{\Psi}(k+1\,|\,k+1) \triangleq -[\hat{\boldsymbol{\psi}}(k+1\,|\,k+1)\times] \tag{63}$$

and where $\hat{\boldsymbol{\psi}}(k+1\,|\,k+1) \triangleq \hat{\boldsymbol{\omega}}(k+1\,|\,k+1) - T\hat{\dot{\boldsymbol{\omega}}}(k+1\,|\,k+1)$ and $\hat{D}^*(k\,|\,k)$ is the a posteriori, orthogonalized estimate of the attitude matrix at time t_k, to be discussed in the sequel.

Finally, because the a posteriori attitude matrix, $\hat{D}(k+1\,|\,k+1)$, is computed based on the a posteriori estimate, $\hat{\boldsymbol{\theta}}(k+1\,|\,k+1)$, this implies a full reset control[22] of the parameter vector, i.e.,

$$\boldsymbol{\theta}^c(k+1) = \boldsymbol{\theta}(k+1) - \hat{\boldsymbol{\theta}}(k+1\,|\,k+1) \tag{64}$$

where $\boldsymbol{\theta}^c(k+1)$ is the reset state vector at t_{k+1} and a corresponding reset of the state estimate

$$\hat{\boldsymbol{\theta}}^c(k+1\,|\,k+1) = 0 \tag{65}$$

which is then used in the ensuing time propagation step.

Remark 4. Notice that, because the reset control is applied to both the state vector and its estimate, no changes are necessary in the estimation error covariance matrix.

Attitude Matrix Orthogonalization

To improve the algorithm's accuracy and enhance its stability, an additional orthogonalization procedure is introduced into the estimator, following the measurement update stage. In this procedure, the orthogonal matrix closest to the filtered attitude matrix is computed.

Given the filtered attitude matrix $\hat{D}(k+1\,|\,k+1)$, the matrix orthogonalization problem is to find the matrix

$$\hat{D}^*(k+1\,|\,k+1) \triangleq \arg\min_{D \in \mathbb{R}^{3,3}} \|\hat{D}(k+1\,|\,k+1) - D\|_F \tag{66a}$$

subject to

$$D^T D = I, \qquad \det D = +1 \tag{66b}$$

where $\|\ \|_F$ is the Frobenius matrix norm.

The matrix orthogonalization problem can be easily solved using the singular value decomposition (SVD)[23] as follows. Let

$$\hat{D}(k+1\,|\,k+1) = U(k+1)\Sigma(k+1)V^T(k+1) \tag{67}$$

be the SVD of $\hat{D}(k+1\,|\,k+1)$, where $U(k+1)$ and $V(k+1)$ are the left and right singular vector matrices, respectively, and $\Sigma(k+1)$ is the singular value matrix. Then

$$\hat{D}^*(k+1\,|\,k+1) = U(k+1) \times \operatorname{diag}\{1,\, 1,\, \det U(k+1)\det V(k+1)\}V^T(k+1) \tag{68}$$

The excessive computational burden associated with the SVD might render its use prohibitive in certain applications, e.g., in real-time attitude determination and control. In such cases, an iterative, fast orthogonalization scheme, introduced in Ref. 24, can be used. Using a single step of this iteration, an improved (nearly orthogonal), a posteriori estimate of the attitude matrix, is computed as

$$\hat{D}^*(k+1\,|\,k+1) = N(k+1)\hat{D}(k+1\,|\,k+1) \tag{69}$$

where the linear transformation that maps the a posteriori attitude matrix into its orthogonalized version is

$$N(k+1) \triangleq \tfrac{3}{2}I - \tfrac{1}{2}\hat{D}(k+1\,|\,k+1)\hat{D}^T(k+1\,|\,k+1) \tag{70}$$

Remark 5. As presented, the orthogonalization step is performed after each measurement update. However, in practice it was found that using the orthogonalization procedure also after the time propagation step, during the filter transient period, improves the filter's convergence rate.

Remark 6. The introduction of the external orthogonalization step into the estimator may, conceivably, affect its statistical characteristics, thus calling for appropriate adjustments in the algorithm to preserve its theoretical properties. However, using an approach similar to that used in Ref. 16, it can be shown that, to first-order accuracy, the orthogonalization procedure does not affect the estimator.

Time Propagation

In the prediction step at t_k, the reset a posteriori estimate at time t_k, $\hat{\boldsymbol{x}}^c(k\,|\,k)$ [computed with the reset IRP estimate according to Eq. (65)] and its corresponding error covariance matrix $P(k\,|\,k)$ are propagated to time t_{k+1}.

Using Eq. (26), we have

$$\hat{\boldsymbol{x}}(k+1\,|\,k) = \Phi(T)\hat{\boldsymbol{x}}^c(k\,|\,k) \tag{71}$$

Using this result with Eq. (26) yields the covariance propagation equation

$$P(k+1\,|\,k) = \Phi(T)P(k\,|\,k)\Phi^T(T) + \Gamma(T)Q(k)\Gamma^T(T) \tag{72}$$

To propagate the attitude matrix to t_{k+1}, we use the most recent IRP, attitude-rate and angular acceleration estimates, and the orthogonalized DCM estimate corresponding to t_k, in Eq. (17). This yields

$$\begin{aligned}\hat{D}(k+1\,|\,k) = \Big\{ & I + \bar{A}(k+1,k) + \tfrac{1}{2}\bar{A}^2(k+1,k) \\ & + \tfrac{1}{6}\bar{A}^3(k+1,k) + \tfrac{1}{6}T[\bar{A}(k+1,k)\hat{\Psi}(k+1\,|\,k) \\ & - \hat{\Psi}(k+1\,|\,k)\bar{A}(k+1,k)]\Big\}\hat{D}^*(k\,|\,k)\end{aligned} \tag{73}$$

where the a priori estimates of $A(k+1,k)$ and $\Psi(k+1)$ are defined as

$$\bar{A}(k+1,k) \triangleq -[\hat{\boldsymbol{\theta}}(k+1\,|\,k)\times] \tag{74}$$

$$\hat{\Psi}(k+1\,|\,k) \triangleq -[\hat{\boldsymbol{\psi}}(k+1\,|\,k)\times] \tag{75}$$

Numerical Example

To demonstrate the performance of the new estimator, a numerical simulation study was performed. Simulating the unitized output of complete vector sensors that measure all three vector components, e.g., magnetometers, the measurements were generated according to the following procedure. At each measurement epoch, a reference-frame modeled (true) unit observation was randomly generated, and the corresponding true body-frame observation was computed using Eq. (31). Zero-mean, white Gaussian measurement noise, orthogonal to the true observation directions, was then added to these observations. The unitized noisy observations then satisfied Eqs. (33) and (35), with $R_v = \sigma_v^2 I$ and $R_u = \sigma_u^2 I$, where the noise equivalent angles were $\sigma_u = \sigma_v = 5$ arcsec. The initial attitude matrix estimate was set to the identity matrix (thus assuming that the body and reference coordinate systems coincide at t_0), while the true attitude corresponded to the 3–2–1 Euler angle rotation sequence of $\phi_3 = 10$, $\phi_2 = 20$, and $\phi_1 = 30$ deg, where ϕ_i is the Euler angle rotation about body axis i. The true angular rate of the body coordinate system relative to the reference coordinate system was set to

$$\boldsymbol{\omega}(t) = \begin{bmatrix} 0.02\sin((2\pi/85)t + (\pi/4)) \\ 0.05\sin((2\pi/45)t + (\pi/2)) \\ 0.03\sin((2\pi/65)t + (3\pi/4)) \end{bmatrix} \text{deg/s} \tag{76}$$

(i.e., the angular velocity's direction was time varying), while the initial angular rate estimates were all set to zero. The filter was run at a rate of 20 Hz, i.e., the sampling interval was $T = 0.05$ s, while the measurement processing rate was 10 Hz. The angular acceleration model parameters were set to: $\tau = 10$ s, $\dot{\omega}_M = 10^{-4}$ rad/s^2, $p_M = p_0 = 0.001$ for all three axes.

To quantify the attitude estimation accuracy using a scalar measure, the attitude error angle is defined as the rotation angle that maps the true attitude to the estimated attitude. This angle, whose statistical properties were discussed in Ref. 25, can be expressed as[26]

$$\varphi(k) = 2\arcsin\left(\frac{\|\hat{D}^*(k\,|\,k) - D(k)\|_F}{\sqrt{8}}\right) \tag{77}$$

In a similar manner, the attitude-rate estimation error is assessed using the following scalar rate error measure:

$$\eta(k) \triangleq \|\hat{\boldsymbol{\omega}}(k\,|\,k) - \boldsymbol{\omega}(k)\| \tag{78}$$

To further demonstrate the performance of the new algorithm, the same numerical example was also run with the attitude and attitude-rate estimation algorithms used in the gyroless SAMPEX spacecraft.[3] (SAMPEX, the first of NASA's new small explorer series, was launched on July 3, 1992, carrying four instruments designed to measure energetic nuclei and electrons over a broad dynamic range.) The SAMPEX estimator is briefly described in the following.

SAMPEX Attitude/Attitude-Rate Estimator

In the SAMPEX attitude control system, the attitude matrix is estimated using the TRIAD[27] algorithm. Thus, if $\boldsymbol{v}_1$ and $\boldsymbol{v}_2$ are two unit vector measurements resolved in the body coordinate system and $\boldsymbol{u}_1$ and $\boldsymbol{u}_2$ are the corresponding unit measurements resolved in the reference coordinate system, then the TRIAD attitude matrix is

$$\hat{D}_{\text{TR}} = VU^T \tag{79}$$

where the matrices V and U are defined as

$$V \triangleq \begin{bmatrix} \boldsymbol{v}_1 & \dfrac{\boldsymbol{v}_1 \times \boldsymbol{v}_2}{\|\boldsymbol{v}_1 \times \boldsymbol{v}_2\|} & \dfrac{\boldsymbol{v}_1 \times (\boldsymbol{v}_1 \times \boldsymbol{v}_2)}{\|\boldsymbol{v}_1 \times \boldsymbol{v}_2\|} \end{bmatrix} \tag{80}$$

$$U \triangleq \begin{bmatrix} \boldsymbol{u}_1 & \dfrac{\boldsymbol{u}_1 \times \boldsymbol{u}_2}{\|\boldsymbol{u}_1 \times \boldsymbol{u}_2\|} & \dfrac{\boldsymbol{u}_1 \times (\boldsymbol{u}_1 \times \boldsymbol{u}_2)}{\|\boldsymbol{u}_1 \times \boldsymbol{u}_2\|} \end{bmatrix} \tag{81}$$

The angular velocity is estimated by averaging the off-diagonal entries of the angular velocity cross-product matrix, computed using the kinematic attitude evolution equation

$$[\hat{\boldsymbol{\omega}}(k)\times] = -\hat{\dot{D}}_{\text{TR}}(k)\hat{D}_{\text{TR}}^T(k) \tag{82}$$

where the attitude matrix rate is estimated using the finite difference scheme

$$\hat{\dot{D}}_{\text{TR}}(k) = \frac{\hat{D}_{\text{TR}}(k) - \hat{D}_{\text{TR}}(k-1)}{T} \tag{83}$$

Remark 7. Notice that the SAMPEX estimator is designed to operate on two vector measurement pairs at each update, whereas the new estimator requires no more than one pair at each update. In the simulations performed in this study, the SAMPEX algorithm was indeed run on twice the amount of data used by the new algorithm.

Results

Figure 1 shows the true Euler angle time histories for the simulation run. These angles were computed from the true attitude matrix (assuming, according to the convention adopted at the beginning of this section, a 3–2–1 Euler angle sequence). Figure 2 shows the time histories of the attitude error angle, defined in Eq. (77), for both the TRIAD method and the new algorithm. Whereas the TRIAD algorithm, which is a point estimation algorithm, has no convergence period, it takes the new filter about 10 s to converge (from the grossly erroneous initial attitude assumed); however, its steady-state performance is clearly much better than that of the TRIAD

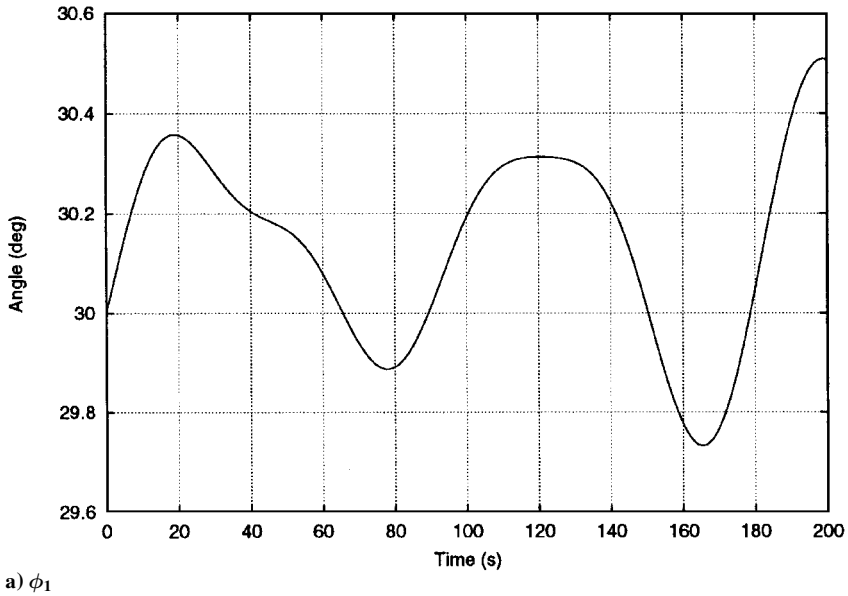

a) ϕ_1

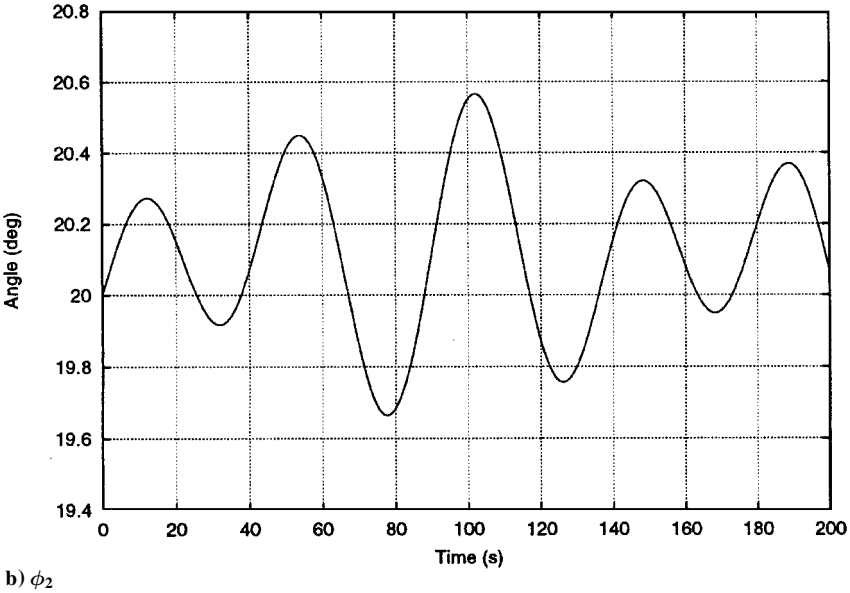

b) ϕ_2

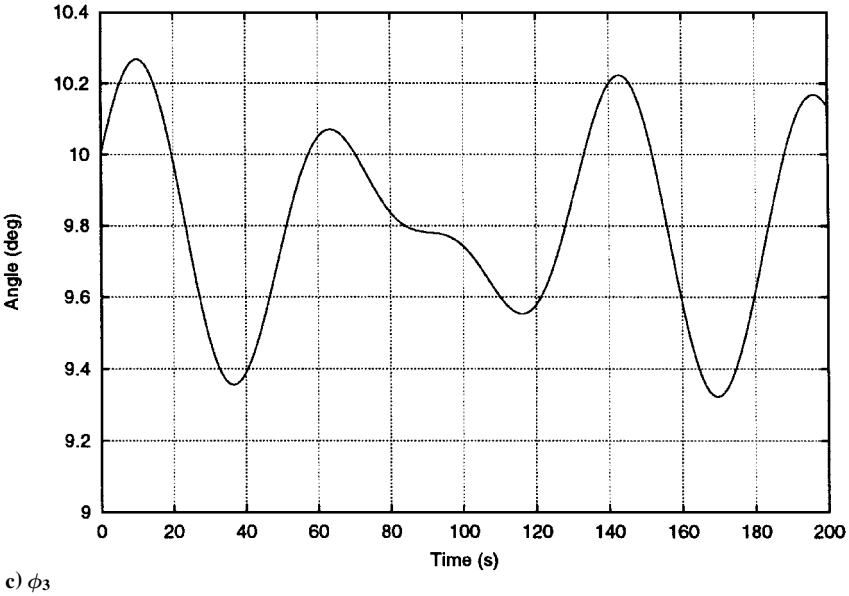

c) ϕ_3

Fig. 1 True Euler angle time histories.

algorithm. Figure 3 presents the time histories of the rate error measure, defined in Eq. (78), for both the SAMPEX rate estimator and the new algorithm. Again, and even more than in the case of the attitude error angle, it is clearly seen that after the new estimator's convergence period (of about 10 s), its performance surpasses by far the performance of the SAMPEX rate estimator. In addition to the earlier mentioned fact that the SAMPEX rate estimator is a memoryless algorithm, the inferior performance of this estimator can be attributed to its use of derivatives of noisy vector measurements, which implies amplification of the measurement noise (the inherent noise amplification associated with differentiation of noisy measurements is independent of the order of the numerical differentiation scheme used). In comparison, the new estimator directly processes the vector measurements to generate attitude-rate estimates.

Using Figs. 2 and 3 to compare the estimation performance of the new algorithm to the performance of the corresponding algorithms implemented in the SAMPEX attitude control system, and noting that the new algorithm used only half the number of vector measurements processed by the SAMPEX estimator, the superiority of the new estimator becomes evident. This should come as no surprise, though, because the SAMPEX estimators are just memoryless point estimation (deterministic) algorithms.

To further demonstrate the performance of the new estimator, the steady-state estimation error standard deviations of the three Euler angles, i.e., the angles computed from the estimated attitude matrix assuming a 3–2–1 rotation sequence, and the three angular velocity components, are compared in Table 1 for both the new algorithm and the SAMPEX estimator. (Actual plots of the Euler angle and rate estimation error time histories are presented in Ref. 28.) As can clearly be observed from Table 1, the new algorithm's Euler angle estimation error standard deviations are about three times smaller than those of the TRIAD algorithm, whereas the rate estimation error standard deviations are more than an order of magnitude smaller than the corresponding SAMPEX estimator's values.

Table 1 Steady-state estimation error standard deviations of new algorithm and SAMPEX estimator

Error	SAMPEX estimator	New algorithm
ϕ_1, arcsec	8.9	2.9
ϕ_2, arcsec	9.2	3.1
ϕ_3, arcsec	8.5	2.9
ω_1, arcsec/s	114.6	3.2
ω_2, arcsec/s	119.0	5.0
ω_3, arcsec/s	126.2	3.1

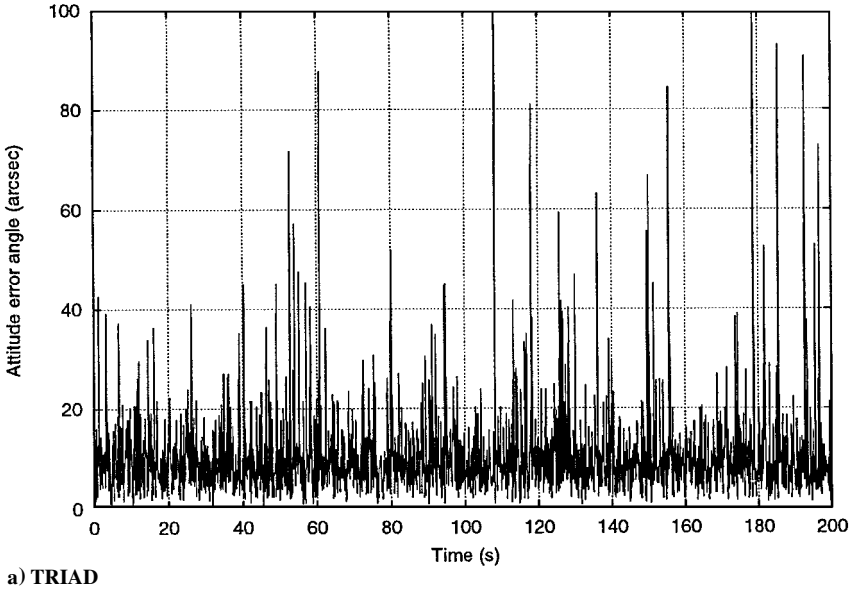

a) TRIAD

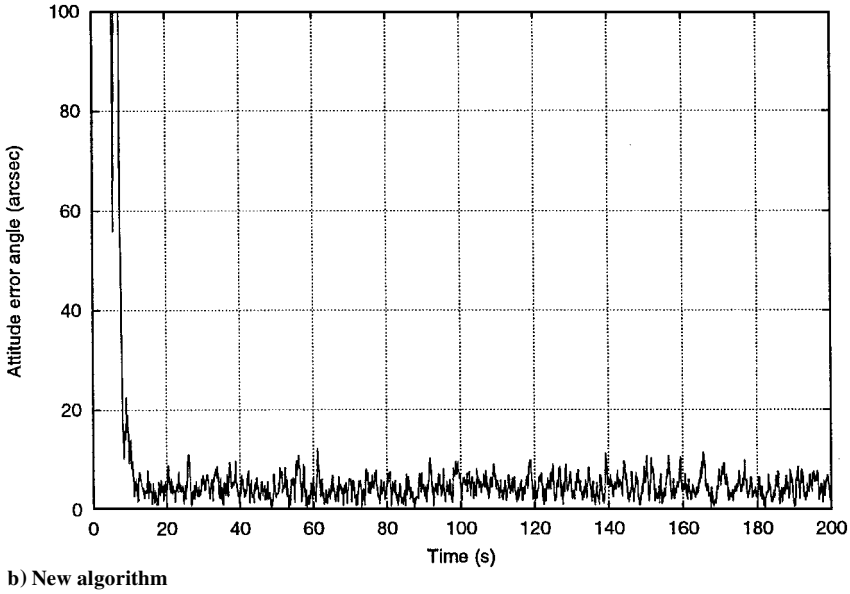

b) New algorithm

Fig. 2 Attitude error angle: new algorithm vs TRIAD.

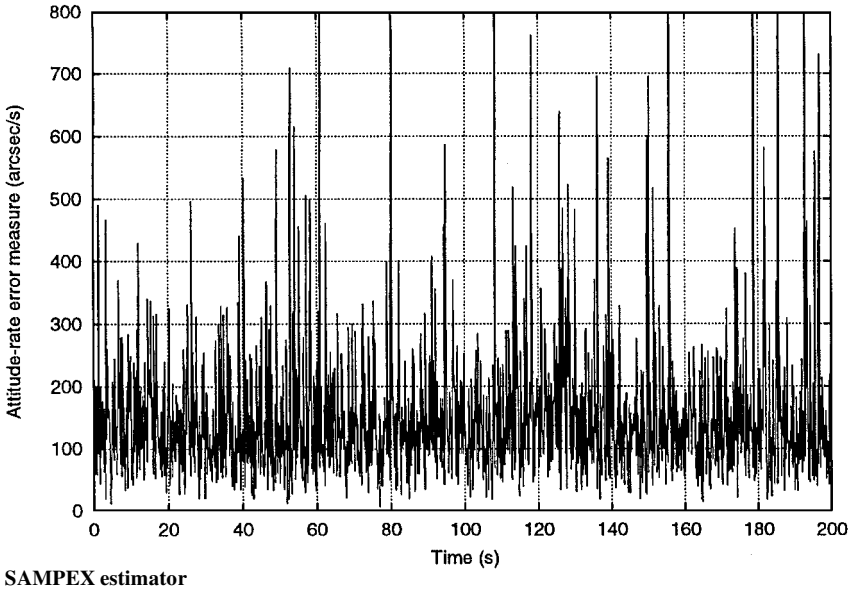

a) SAMPEX estimator

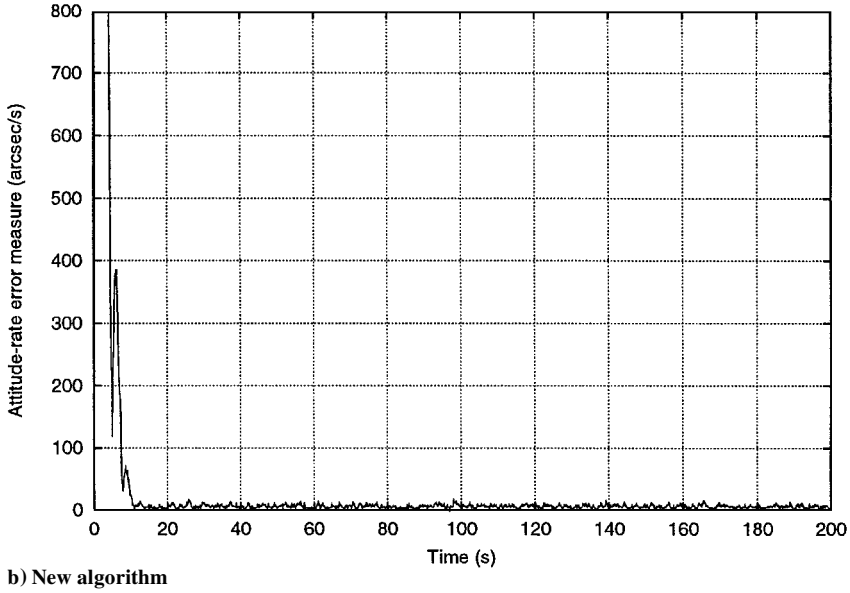

b) New algorithm

Fig. 3 Attitude rate error measure: new algorithm vs the SAMPEX estimator.

Conclusions

A computationally efficient, nonlinear estimator has been presented that directly uses vector measurements to estimate both the attitude matrix and the angular velocity, avoiding precomputation of the temporal derivatives of these noisy measurements. The algorithm is based on the IRP third-order minimal parameterization of the attitude matrix, which is at the heart of its computational efficiency. Avoiding the use of the uncertain spacecraft dynamic model, the filter uses a polynomial state-space model, in which the spacecraft angular acceleration is modeled as an exponentially autocorrelated stochastic process, a concept borrowed from tracking theory. Although the kinematic model used in this study was a simple, decoupled one, the method can be easily extended if needed to include more complex, coupled models, to track high-dynamics spacecraft. Moreover, adaptive estimation algorithms can be used to identify the parameters of the filter online.

Simulations demonstrate the viability, accuracy, and robustness of the new algorithm. In particular, the performance of the estimator has been shown to be superior to the performance of the attitude/attitude-rate estimator implemented in the SAMPEX spacecraft.

Acknowledgments

This work was performed while the first author held a National Research Council–NASA Goddard Space Flight Center Senior Research Associateship. The authors would like to express their thanks to the reviewers, whose comments helped improve the paper.

References

[1]Lefferts, E. J., Markley, F. L., and Shuster, M. D., "Kalman Filtering for Spacecraft Attitude Estimation," *Journal of Guidance, Control, and Dynamics*, Vol. 5, No. 5, 1982, pp. 417–429.

[2]Kudva, P., and Throckmorton, A., "Attitude Determination Studies for the Earth Observation System AM1 (EOS-AM1) Mission," *Journal of Guidance, Control, and Dynamics*, Vol. 19, No. 6, 1996, pp. 1326–1331.

[3]Flatley, T. W., Forden, J. K., Henretty, D. A., Lightsey, E. G., and Markley, F. L., "On-Board Attitude Determination and Control Algorithms for SAMPEX," *Proceedings of Flight Mechanics/Estimation Theory Symposium*, NASA CP 3102, NASA Goddard Space Flight Center, Greenbelt, MD, 1990, pp. 379–398.

[4]Chu, D., Glickman, J., and Harvie, E., "Improvements in ERBS Attitude Determination Without Gyros," *Proceedings of Flight Mechanics/Estimation Theory Symposium*, NASA CP 3186, NASA Goddard Space Flight Center, Greenbelt, MD, 1992, pp. 185–200.

[5]Gai, E., Daly, K., Harrison, J., and Lemos, L., "Star-Sensor-Based Satellite Attitude/Attitude Rate Estimator," *Journal of Guidance, Control, and Dynamics*, Vol. 8, No. 5, 1985, pp. 560–565.

[6]Challa, M. S., Natanson, G. A., Baker, D. F., and Deutschmann, J. K., "Advantages of Estimating Rate Corrections During Dynamic Propagation of Spacecraft Rates—Applications to Real-Time Attitude Determination of SAMPEX," *Proceedings of Flight Mechanics/Estimation Theory*

Symposium, NASA CP 3265, NASA Goddard Space Flight Center, Greenbelt, MD, 1994, pp. 481–495.

[7]Azor, R., Bar-Itzhack, I. Y., and Harman, R. H., "Satellite Angular Rate Estimation from Vector Measurements," *Journal of Guidance, Control, and Dynamics*, Vol. 21, No. 3, 1998, pp. 450–457.

[8]Algrain, M. C., and Saniie, J., "Interlaced Kalman Filtering of 3-D Angular Motion Based on Euler's Nonlinear Equations," *IEEE Transactions on Aerospace and Electronic Systems*, Vol. 30, No. 1, 1994, pp. 175–185.

[9]Crassidis, J. L., and Markley, F. L., "Predictive Filtering for Attitude Estimation Without Rate Sensors," *Journal of Guidance, Control, and Dynamics*, Vol. 20, No. 3, 1997, pp. 522–527.

[10]Lefferts, E. J., and Markley, F. L., "Dynamic Modeling for Attitude Determination," AIAA Paper 76-1910, Aug. 1976.

[11]Mook, D. J., De Pena, J., Crassidis, J. L., and Meyer, T. J., "Dynamics-Based Robust Attitude Estimation," *Proceedings of the AAS/AIAA Astrodynamics Specialist Conference* (Victoria, BC, Canada), American Astronautical Society, San Diego, CA, 1993, pp. 39–58; also American Astronautical Society Paper 93-554, Aug. 1993.

[12]Psiaki, M. L., Martel, F., and Pal, P. K., "Three Axis Attitude Determination via Kalman Filtering of Magnetometer Data," *Journal of Guidance, Control, and Dynamics*, Vol. 13, No. 3, 1990, pp. 506–514.

[13]Ronen, M., and Oshman, Y., "A Third-Order, Minimal-Parameter Solution of the Orthogonal Matrix Differential Equation," *Journal of Guidance, Control, and Dynamics*, Vol. 20, No. 3, 1997, pp. 516–521.

[14]Singer, R. A., "Estimating Optimal Tracking Filter Performance for Manned Maneuvering Targets," *IEEE Transactions on Aerospace and Electronic Systems*, Vol. AES-6, No. 4, 1970, pp. 473–483.

[15]Wertz, J. R. (ed.), *Spacecraft Attitude Determination and Control*, D. Reidel, Dordrecht, The Netherlands, 1978, Chap. 13.

[16]Oshman, Y., and Markley, F. L., "Minimal-Parameter Attitude Matrix Estimation from Vector Observations," *Journal of Guidance, Control, and Dynamics*, Vol. 21, No. 4, 1998, pp. 595–602.

[17]Challa, M., Natanson, G., and Wheeler, C., "Simultaneous Determination of Spacecraft Attitude and Rates Using Only a Magnetometer," *Proceedings of the AIAA/AAS Astrodynamics Specialist Conference* (San Diego, CA), AIAA, Reston, VA, 1996, pp. 544–553 (AIAA Paper 96-3630).

[18]Oshman, Y., and Bar-Itzhack, I. Y., "Eigenfactor Solution of the Matrix Riccati Equation—A Continuous Square Root Algorithm," *IEEE Transactions on Automatic Control*, Vol. AC-30, No. 10, 1985, pp. 971–978.

[19]Chang, C. B., and Tabaczynski, J. A., "Application of State Estimation to Target Tracking," *IEEE Transactions on Automatic Control*, Vol. AC-29, No. 2, 1984, pp. 98–109.

[20]Zhou, H., and Kumar, K. S. P., "A 'Current' Statistical Model and Adaptive Algorithm for Estimating Maneuvering Targets," *Journal of Guidance, Control, and Dynamics*, Vol. 7, No. 5, 1984, pp. 596–602.

[21]Mazor, E., Averbuch, A., Bar-Shalom, Y., and Dayan, J., "Interacting Multiple Model Methods in Target Tracking: A Survey," *IEEE Transactions on Aerospace and Electronic Systems*, Vol. 34, No. 1, 1998, pp. 103–123.

[22]Maybeck, P. S., *Stochastic Models, Estimation and Control*, Vol. 1, Academic, New York, 1979, pp. 334–336.

[23]Markley, F. L., "Attitude Determination Using Vector Observations and the Singular Value Decomposition," *Journal of the Astronautical Sciences*, Vol. 36, No. 3, 1988, pp. 245–258.

[24]Bar-Itzhack, I. Y., and Meyer, J., "On the Convergence of Iterative Orthogonalization Processes," *IEEE Transactions on Aerospace and Electronic Systems*, Vol. AES-12, No. 2, 1976, pp. 146–151.

[25]Mortari, D., Pollock, T. C., and Junkins, J. L., "Towards the Most Accurate Attitude Determination System Using Star Trackers," 8th AAS/AIAA Space Flight Mechanics Meeting, American Astronautical Society Paper 98-159, Monterey, CA, 1998.

[26]Markley, F. L., "Attitude Determination Using Vector Observations: A Fast Optimal Matrix Algorithm," *Journal of the Astronautical Sciences*, Vol. 41, No. 2, 1993, pp. 261–280.

[27]Black, H. D., "A Passive System for Determining the Attitude of a Satellite," *AIAA Journal*, Vol. 2, No. 7, 1964, pp. 1350, 1351.

[28]Oshman, Y., and Markley, F. L., "Sequential Gyroless Attitude/Attitude-Rate Estimation Using Integrated-Rate Parameters," AIAA Paper 98-4508, Aug. 1998.